ELSEVIER

Contents lists available at ScienceDirect

Results in Chemistry

journal homepage: www.sciencedirect.com/journal/results-in-chemistry





Evaluation of the corrosion inhibition efficiency of 7-(Acetohydrazide-2-yloxy)-4-methylcoumarin in 1.0 M HCl: Experimental and theoretical approach

Ali H.A. Kareem ^a, Hakim S. Aljibori ^b, Ahmed Alamiery ^{c,d,*}, Lina M. Shaker ^d

- ^a Department of Production Engineering and Metallurgical, University of Technology, Baghdad 10001, Iraq
- ^b College of Engineering, University of Warith Al-Anbiyaa, Karbalaa, Iraq
- ^c Al-Ayen University (AUIQ), Nile St, Nasiriyah, Dhi Qar, Iraq
- d Department of Chemical and Process Engineering, Faculty of Engineering and Built Environment, Universiti Kebangsaan Malaysia, Bangi, Malaysia

ARTICLE INFO

Keywords: Corrosion DFT EIS Methylcoumarin And HCl

ABSTRACT

This study investigates the corrosion inhibition potential of 7-(acetohydrazide-2-yloxy)-4-methylcoumarin (AMC) in 1.0 M HCl, emphasizing its efficiency at varying concentrations. The inhibitory performance was evaluated using potentiodynamic polarization and electrochemical impedance spectroscopy (EIS) to assess the effectiveness of AMC's in mitigating mild steel corrosion. The results revealed that AMC exhibited a peak inhibition efficiency of 90.7 % at 0.5 mM, demonstrating its exceptional protective ability. The adsorption process was found to follow the Langmuir model, confirming the formation of a stable monolayer on metal surface. To gain deeper insights into the inhibition mechanism, Density Functional Theory (DFT) calculations were performed, revealing key electronic structure parameters and adsorption behavior of AMC at the molecular level. The findings highlight AMC a highly efficient and environmentally viable corrosion inhibitor in HCl solution, offering strong adsorption capabilities and long-term stability.

1. Introduction

Corrosion significantly impacts various industry sectors, particularly those operating under acidic conditions [1-3]. One of the most successful and cost-effective techniques for reducing corrosion is the use of corrosion inhibitors [4,5]. Corrosion inhibitors can be classified broadly as inorganic and organic. The inorganic inhibitors, commonly known to contain chromium, molybdenum, and nitrites, are capable of providing effective passive film protection on the surfaces of metals [6,7]. However, the health and environmental issues that some inorganic inhibitors pose have intensified research efforts for the so-called greener, safer alternatives. Organic inhibitors, characterized by their diverse chemical structures, have received considerable attention due to their high efficiency and eco-friendliness. Compounds containing nitrogen (N), oxygen (O), sulfur (S), and phosphorus (P) atoms have been found with excellent corrosion inhibition properties by the formation of stable complexes with metal surfaces [8–10]. Among these, a promising class of organic inhibitors includes coumarin derivatives [11–13]. Coumarins are compounds containing a benzene ring together with an α -pyrone moiety and have multiple functionalities, resulting in strong adsorption onto metal surfaces, thus reducing corrosion [14–16]. Within corrosion science, Density Functional Theory (DFT) has become an invaluable computational tool in understanding the molecular mechanisms of corrosion inhibition.

The metal structures might be said to be significantly exposed because of the presence of thin electrolyte films and exposure to corrosive gases on the metallic surface. The possibility for the transformation of metallic particles to oxide or salt structures is high in moisture conditions. More specifically, for metals such as steel, the presence of ionic moisture content creates a situation that is very dangerous for the metal structures during the corrosion attack [17,18]. Corrosion occurs due to the differences in chemical compositions on different parts of the metal surface. Thus, it can be concluded that metallic surfaces in structural and construction applications are exposed to saline, acidic, or alkaline moisture which creates conditions that accelerate the significant economic losses caused by corrosion. A classic

E-mail address: dr.ahmed1975@ukm.edu.my (A. Alamiery).

^{*} Corresponding author at: Department of Chemical and Process Engineering, Faculty of Engineering and Built Environment, Universiti Kebangsaan Malaysia, Bangi, Malaysia

example is the introducing of bent steel metals from salty water or dry spaces into an environment with humid or moister conditions, bringing about corrosion effects on the steel metals. Such conditions can bring about localized corrosion in metal materials because of barriers formed at local spots where small moisture can collect. These localized areas do not come into the full air zone when the area with moisture is covered. If such conditions are aggravated with poor drainage systems, local cathodic and possibly hydrogen sulfide systems can evolve with barriers within metals [19-21]. The DFT has a lot of depth in inhibitor-metal interaction in terms of electronic structures then adsorption energies and charge transfer processes. All these features then allow the rational design of newer inhibitors possessing better performances [22-24]. Whereas significant advancements in the field of corrosion inhibition have been noted, an exploration still has to be on the new inhibitor molecules as well as assessing their action in different conditions. Therefore, this research looks into the efficiency of inhibition against corrosion of AMC, which is an example of a derivative of coumarins, on mild steel when it is in an acidic medium. This study combines both experimentation and theoretical calculations in the field of development and formulation of simple as well as environmental-friendly corrosion

New corrosion inhibitors need to be developed because the corrosion problem is still very active in many industries. Significant corrosion, for example, due to acidic action, is still damaging metals, causing failures in strength, revenue losses, and loss of safety. While conventional inhibitors have been widely used for many years, numerous inorganic inhibitors are damaging to health and the environment, making them a less attractive choice to be used for their particular purposes. This interest is now growing into organic inhibitors which are safer and often more environmentally friendly, however, their efficiency and applicability require further exploration in terms of efficiency and application under varying conditions. Therefore, there is a critical need to find and formulate new inhibitors that would be useful in corrosion protection but also fulfill environmental and economic sustainability criteria. This gap can be fulfilled with the help of understanding new corrosionresistant compounds and using advanced techniques for rational understanding of their inhibition mechanisms. The current study addresses one major gap regarding corrosion inhibition performance of AMC in a 1.0 M HCl solution. With the systematic examination of AMC concentration effects on inhibition efficiency, this study aims to give rich insight into the anticorrosion potential application of AMC. Experimental methods that include potentiodynamic polarization (PDP) curves and electrochemical impedance spectroscopy (EIS) coupled to theoretical knowledge from Density Functional Theory (DFT) calculations provide a comprehensive angle on the corrosion inhibition mechanism of AMC (Fig. 1). Such understanding will favor advancements in the field of corrosion science and engineering.

2. Materials and methods

1.1. Synthesis of Inhibitor

The inhibitor, AMC was synthesized following the methodology described by Hamdi et al. [25].

Fig. 1. The chemical structure of AMC.

2.1. Materials

Mild steel coupons obtained from Metal Samples Company, were used as the working electrodes in the current investigation. The chemical composition of the mild steel coupons, presented in weight percentage, is presented in Table 1. Before experimentation, the mild steel coupons were cleaned according to the standard method G1–03/ASTM [26,27].

The working electrode used was a mild steel sample with dimensions of 1 cm \times 1 cm. The electrode surface was polished sequentially using silicon carbide abrasive papers of different grades (from 400 to 1200 grit) to obtain a mirror-like surface. After polishing, the electrode was with distilled water, degreased with acetone, and dried. The pre-treated electrode was then immediately immersed in the test solution to prevent contamination. A 1.0 M HCl solution was prepared using analyticalgrade hydrochloric acid and distilled water. AMC was prepared in the acidic solution at varying concentrations (0.1, 0.2, 0.3, 0.4, and 0.5 mM) to study its inhibition performance. The working electrode was immersed in the test solution containing AMC for 30 min before measurements to ensure the formation of an adsorption layer on the electrode surface. All experiments were performed under controlled temperature conditions of 303 K using a thermostatic water bath. After each measurement, the electrodes were carefully removed, rinsed with distilled water, dried, and stored in a desiccator for subsequent analysis.

2.2. Electrochemical measurements

Electrochemical impedance spectroscopy (EIS) measurements were conducted in aerated, unstirred 1.0 M HCl solutions containing various concentrations of the inhibitor. These measurements were performed at steady-state corrosion potential using a Gamry water-jacketed glass cell equipped with three electrodes: a working electrode (mild steel specimen), a counter electrode (graphite bar), and a reference electrode (saturated calomel electrode, SCE). The electrochemical measurements were carried out using a Gamry REF 600 Potentiostat/Galvanostat/ZRA model and monitored with Gamry's DC105 and EIS300 software. For the EIS experiments, an AC signal with a peak-to-peak amplitude of 5 mV at the corrosion potential was applied over a frequency range of 100 kHz to 0.1 Hz. The impedance data were analyzed and fitted to appropriate equivalent circuits (ECs) using the Gamry Echem Analyst program. To ensure a stable potential, all electrochemical tests were started 30 min after electrode immersion in the solution. Each experiment was repeated three times under identical conditions, and only the average data were reported reproducibility and accuracy of the results [28].

2.3. Density functional theory (DFT) computations

To complement the experimental results, quantum chemical calculations were performed to analyze the electronic structure and chemical reactivity of the AMC molecule. DFT computations were conducted using ChemOffice software, employing Becke's three-parameter hybrid functional (B3LYP) with the Gaussian 03 software and the 6–31G reference basis set. Key quantum chemical parameters, including the energy gap (Δ E), fraction of electron transfer (Δ N), dipole moment (μ), ionization energy (I), electron affinity (A), absolute electronegativity (χ), hardness (η), and softness (σ), were determined for AMC in the gas phase [29–31]. These parameters were calculated using the following equations (Eqs. 1–6):

$$I = -E_{HOMO} \tag{1}$$

$$A = -E_{LUMO} \tag{2}$$

$$\chi = \frac{I+A}{2} \tag{3}$$

Table 1Chemical Composition of Mild Steel Coupons (wt%).

Element	Carbon	Manganese	Silicon	Aluminum	Sulfur	Phosphorus	Iron
Percentage	0.210	0.050	0.380	0.010	0.050	0.090	Balance

$$\eta = \frac{I - A}{2} \tag{4}$$

$$\sigma = \frac{1}{n} \tag{5}$$

$$\Delta N = \frac{\chi_{Fe} - \chi_{inh}}{2(\eta_{Fe} + \eta_{inh})} \tag{6}$$

where χFe is the electronegativity of iron and ηinh is the hardness of iron. It was reported that χ_{Fe} , was of 7 eV/mol, whereas η_{Fe} was 0 eV/mol [31].

3. Results and discussion

3.1. Chemistry

The synthesis of AMC involves a straightforward two-step process, as depicted in Fig. 2. The first step involves the esterification of 7-hydroxy-4-methylcoumarin (compound 1) using ethyl bromoacetate in the presence of anhydrous potassium carbonate (K_2CO_3). Dry acetone is used as the solvent under reflux conditions, ensuring full esterification of the hydroxyl group, yielding intermediate compound 2. Compound (2) undergoes a nucleophilic substitution reaction with hydrazine hydrate (N_2H_4) under reflux, to form the target compound (Fig. 2).

3.2. Electrochemical measurements

3.2.1. Electrochemical impedance spectroscopy (EIS) measurements

The corrosion behavior of mild steel in a 1.0 M HCl solution at 303 K both in the absence and presence of varying concentrations of AMC was analyzed through Electrochemical Impedance Spectroscopy (EIS). The Nyquist plots, presented in Fig. 3, display a series of semicircles, characteristic of electrochemical processes at the metal-solution interface. The diameter of each semicircle is directly correlated with the charge transfer resistance (Rct), a critical parameter for evaluating corrosion inhibition efficiency. The experimental data, summarized in Table 2, demonstrate that AMC addition significantly enhances impedance, signifying improved corrosion resistance of mild steel. This enhancement results from the formation of a protective adsorption layer on the metal surface, effectively mitigating the corrosive effects of HCl. The inhibition efficiency (IE%) of AMC was calculated using Eq. (7):

$$IE(\%) = \frac{R_{ct}^o - R_{ct}}{R_{ct}^o} \times 100$$
 (7)

Where R_{ct}^o and R_{ct} are the charge transfer resistances in the absence and presence of AMC, respectively.

As presented in Table 2, inhibition efficiency increases with rising AMC concentration. Specifically, the efficiency improves from 83.1 % at 0.1 mM to 89.5 % at 0.5 mM. This trend underscores the high performance of AMC as a corrosion inhibitor, particularly at elevated concentrations. The findings confirm that AMC effectively establishes a stable and protective adsorption layer protective barrier on the metal surface, significantly reducing the corrosion rate [32–34].

As shown in Table 2, the charge transfer resistance (R_{ct}) values increase with elevated AMC concentrations. The Nyquist plots in Fig. 3 exhibit well-defined semicircles, whose diameters expand progressively with increasing AMC concentrations. This behavior confirms that AMC improves charge transfer resistance, thereby reducing the corrosion rate [34].

The capacitive behavior of the double layer at the metal-solution interface is represented by Constant Phase Element (CPE_{dl}) in the equivalent circuit model schematically illustrated in Fig. 4. This model was employed to fit the impedance data, providing a realistic representation of the electrochemical processes occurring at the interface [35]

From this perspective, EIS results confirm that AMC significantly improves the corrosion resistance of mild steel in 1.0 M HCl, based on EIS results. The increasing Rct values at higher AMC concentrations correspond to increased inhibition efficiencies, reaching a maximum of 89.5 % at 0.5 mM, indicating that it could be an effective corrosion inhibitor for mild steel in acidic environments. Moreover, the Nyquist plots further validate the equivalent circuit model, confirming its ability to accurately capture the electrochemical processes, reinforcing the proposed protective mechanism of AMC.

3.2.2. Polarization measurements

The polarization behavior of mild steel in a 1.0 M HCl solution, with and without various concentrations of AMC, is illustrated in Fig. 5. The polarization curves provide critical insights into the electrochemical processes at the metal surface, particularly the anodic and cathodic reactions governing corrosion [35]. Key polarization parameters derived from the potentiodynamic polarization curves are summarized in Table 3. These include the corrosion current density (icorr), corrosion potential (Ecorr), anodic Tafel slope (β_a), and cathodic Tafel slope (β_c). These parameters were determined by locating the intersection of anodic and cathodic Tafel lines at the corrosion potential. The icorr values quantify the corrosion rate. As shown in Table 3, the presence of AMC significantly decreases icorr, from 644.8 $\mu A/cm^2$ in the absence of

Fig. 2. Synthesis route for AMC.

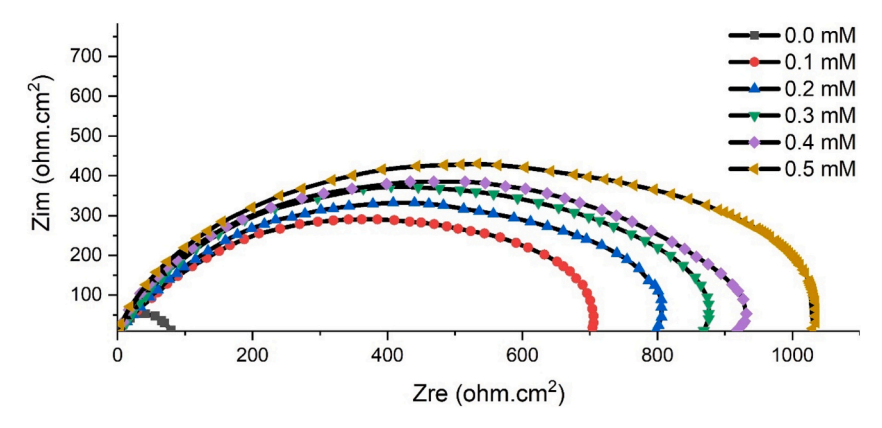


Fig. 3. Nyquist plots of mild steel in 1.0 M HCl solution at varying AMC concentrations at 303 K. The spectra demonstrate an increase in total impedance with AMC concentration indicating enhanced corrosion inhibition at elevated AMC concentrations.

 Table 2

 Inhibition efficiency of AMC determined from electrochemical impedance spectroscopy (EIS) measurements at varying concentrations at 303 K.

C _{inh} (mM) CPE _{dl}			$C_{dl}\left(\mu F.cm^{-2}\right)$	$R_{ct}(\Omega.cm^2)$	$R_s(\Omega.cm^2)$	IE (%)
0.0	$Y_o(\mu S.s^{\alpha}cm^{-2})$	α	129	0.0925	1.944	0.0
0.1	907	0.83	94	0.5483	0.776	83.1
0.2	522	0.77	72	0.6760	0.521	86.3
0.3	492	0.77	59	0.7184	0.474	87.1
0.4	447	0.79	41	0.8345	0.461	88.9
0.5	389	0.82	33	0.8811	0.419	89.5

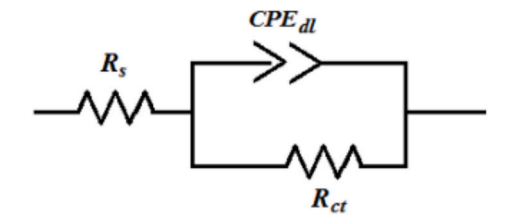


Fig. 4. Equivalent model used to fit the impedance data for mild steel immersed in $1.0\ M$ HCl with and without AMC.

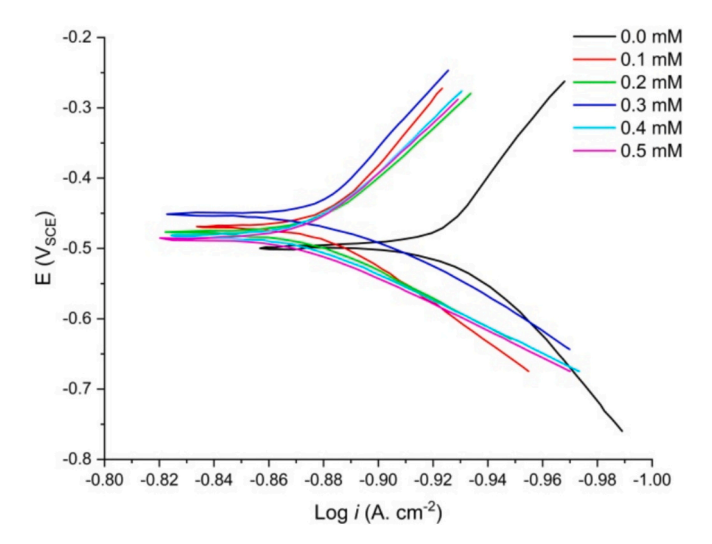


Fig. 5. Potentiodynamic polarization curve for mild steel in 1.0 M HCl with various concentrations of the AMC at 303 K.

Table 3Polarization parameters for mild steel in 1.0 M HCl with different concentrations of the AMC at 303 K.

Conc. (mM)	i _{corr} (μA·cm ⁻²)	E _{CORR} (VSCE)	βa (V·dec ⁻¹)	βc (V·dec ⁻¹)	IE (%)
0	644.8	-0.51	0.15	0.15	0
0.1	216.7	-0.57	0.13	0.14	66.4
0.2	186.3	-0.53	0.15	0.16	71.0
0.3	95.5	-0.52	0.08	0.11	84.2
0.4	73.8	-0.51	0.06	0.09	88.5
0.5	61.1	-0.48	0.05	0.09	90.7

AMC to just $61.1 \,\mu\text{A/cm}^2$ at the highest concentration of $0.5 \,\text{mM}$. This substantial reduction in i_{corr} indicates that AMC effectively inhibits mild steel corrosion in 1.0 M HCl. The progressive decline in icorr with increasing AMC concentration is attributed to the formation of a protective adsorption film on the steel surface, which impedes the electrochemical reactions driving the corrosion process [36]. The Ecorr values provide insights into the electrochemical influence of AMC. As seen in Table 3, the addition of AMC results in a positive shift in Ecorr, from -0.51 V (SCE) in the absence of AMC to -0.48 V (SCE) at 0.5 mM. This positive shift suggests that AMC decreases the electrochemical driving force for anodic metal dissolution, acting as a protective agent. However, since the Ecorr shift is less than 85 mV, AMC can be classified as a mixed-type inhibitor, influencing both anodic and cathodic processes [37]. The Tafel slopes provide information regarding the kinetics of anodic and cathodic reactions. According to Table 3, both β_a and β_c decrease with increasing AMC concentration. Specifically, β_{a} decreases from 0.15 V/dec to 0.05 V/dec, while β_c decreases from 0.15 V/dec to 0.09 V/dec as the AMC concentration increases from 0 mM to 0.5 mM. This indicates that AMC slows both the anodic dissolution of iron and the cathodic reduction of hydrogen ions, effectively inhibiting the overall corrosion process [38]. In conclusion, the polarization measurements confirm that AMC significantly reduces the corrosion rate of mild steel in acidic environments by forming a protective surface layer and acting as a mixed-type inhibitor. This dual functionality makes AMC a promising

candidate for corrosion protection in industrial applications.

The inhibition efficiency (IE%) of AMC was calculated using Eq. (8), where i_{corr} and $i_{corr(inh)}$ represent the corrosion current densities in the absence and presence of AMC, respectively.

$$IE(\%) = \frac{i_{corr} - i_{corr(inh)}}{i_{corr(inh)}} \times 100$$
(8)

The calculated inhibition efficiencies presented in Table 3 demonstrate a significant improvement with increasing AMC concentrations. Starting at 66.4 % efficiency at 0.1 mM, the inhibition efficiency progressively increases, reaching 90.7 % at 0.5 mM. These high inhibition levels highlight AMC's strong ability to protect mild steel from acidinduced corrosion. The potentiodynamic polarization curves in Fig. 5 illustrate that AMC addition affects both the anodic and cathodic branches, leading to a notable shift toward lower current densities as AMC concentration increases. This confirms AMC's dual role in mitigating the rates of anodic and cathodic reactions. The simultaneous reduction in both βa and βc further validates AMC's mixed-type inhibition behavior, effectively controlling metal dissolution (anodic reaction) and hydrogen evolution (cathodic reaction) [39].

In conclusion, the potentiodynamic polarization studies confirm that AMC serves as a highly effective mixed-type inhibitor for the corrosion of mild steel in 1.0 M HCl solution at 303 K. The significant reduction in $i_{\rm corr}$, combined with the positive shift in $E_{\rm corr}$ and the reduction of both anodic and cathodic Tafel slopes, suggests the formation of a stable protective layer on the steel surface. This layer prevents both anodic iron dissolution and cathodic hydrogen evolution reactions, ensuring high inhibition efficiency, particularly at elevated AMC concentrations. The polarization curves and inhibition efficiency data consistently confirm AMC's potential as a highly effective corrosion inhibitor for acidic environments.

3.3. Adsorption isotherm

The adsorption behavior of AMC on the mild steel surface in 1.0 M HCl solution was analyzed using the Langmuir adsorption isotherm model. The plot of C_{inh}/θ versus C_{inh} (Fig. 6) demonstrates a linear relationship with a high correlation coefficient ($R_2=0.9983$), indicating that the adsorption of AMC onto the steel surface closely follows the Langmuir isotherm model [40]. The Langmuir adsorption isotherm is mathematically expressed as Eq. (9):

$$\frac{C_{inh}}{\theta} = \frac{1}{K_{ads}} + C_{inh} \tag{9}$$

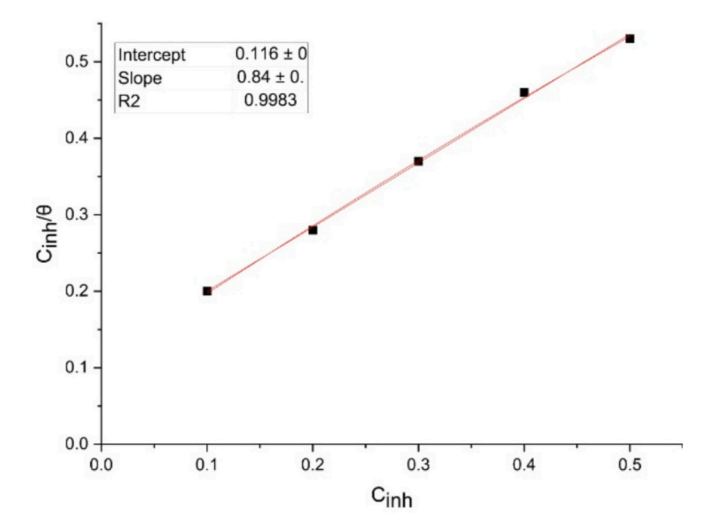


Fig. 6. Langmuir isotherm model

where C_{inh} is the inhibitor concentration, θ denotes the surface coverage, and K_{ads} is the adsorption equilibrium constant.

The linearity of the plot confirms that AMC adsorption occurs via a monolayer adsorption process, where each AMC molecule occupies a specific adsorption site on the metal surface, with minimal interactions between adsorbed molecules [41]. The slope and intercept of the plot were used to determine K_{ads}, with the slope value (0.84) being close to unity, consistent with the Langmuir model assumptions. From the intercept, K_{ads} was calculated, yielding a high adsorption equilibrium constant, indicative of strong adsorption of AMC molecules onto the metal surface. This aligns with electrochemical studies, which reported high inhibition efficiency. The strong adsorption suggests that AMC molecules form chemisorptive interactions with the steel surface, likely through active sites such as oxygen and nitrogen atoms, which coordinate with the vacant d-orbitals of iron atoms in the steel. This robust interaction establishes a stable protective barrier, preventing aggressive ions from infiltrating and attacking the metal surface [42,43]. In summary, the adsorption isotherm analysis confirms that AMC exhibits strong and effective adsorption on the mild steel surface, following the Langmuir isotherm model.

3.4. DFT calculations

The quantum chemical parameters presented in Table 4 provide critical insights into the properties of AMC. The ionization energy of 9.169 eV indicates that AMC exhibits considerable stability, making it less prone to electron loss. This characteristic supports the formation of a durable protective layer on metal surfaces. Additionally, the electron affinity value of 3.950 eV demonstrates AMC's capacity to accept electrons, potentially promoting stronger interactions between the inhibitor and the metal, thereby enhancing adsorption [44-47]. The HOMO energy level is observed at -9.169 eV, while the LUMO is at -3.950 eV, leading to a substantial energy gap (ΔE) of 5.219 eV. A larger energy gap generally corresponds to higher chemical stability and lower reactivity, desirable attributes for corrosion inhibitors as they contribute to the formation of a stable protective barrier on the metal surface. With a hardness value of 2.60 eV, AMC demonstrates moderate resistance to electron cloud deformation, which supports its role as a corrosion inhibitor. The electronegativity of 6.55 eV suggests that AMC can effectively attract electrons from the metal surface, enhancing adsorption. he negative ΔN value (-0.0844 eV) indicates that AMC has a tendency to donate electrons to the metal surface, facilitating the formation of a protective film.

The visual representations of the HOMO and LUMO orbitals (Fig. 7) provide insights into the reactivity of AMC. The HOMO is primarily localized on the oxygen atoms and the coumarin ring, suggesting that these regions play a key role in electron donation to the metal surface, thereby enhancing adsorption. The LUMO, is distributed over the coumarin ring and neighboring atoms, indicating potential electron-accepting sites. This distribution of the frontier molecular orbitals suggests that AMC can effectively interact with the metal surface, providing both electron donation and acceptance capabilities that are crucial for forming a stable and protective adsorption layer [48,49].

The distribution of atomic charges (Fig. 8) derived from the DFT calculations further identifies the reactive sites within the AMC molecule. Significant negative charges are observed on the oxygen atoms, indicating that these atoms are highly prone to interactions with the iron atoms of metal surface. The overall distribution of atomic charges supports the notion that AMC can establish multiple interactions with the metal surface, enhancing the anticorrosion properties of AMC. DFT studies on AMC reveal that its electronic characteristics, such as a large energy gap, favorable hardness, and the arrangement of frontier molecular orbitals, make it highly effective as a corrosion inhibitor [50]. The distribution of atomic charges highlights the reactive centers that facilitate AMC's strong binding to metal surfaces. These results are consistent with the molecule's demonstrated high corrosion inhibition

Table 4
Quantum chemical parameters of AMC corrosion inhibitor, calculated using DFT at the B3LYP basis set in its neutral form.

I(eV)	A(eV)	$E_{HOMO}(eV)$	$E_{LUMO}(eV)$	$\Delta E(eV)$	η	χ	$\Delta N(eV)$
9.169	3.950	-9.169	-3.950	5.219	2.60	6.55	-0.0844

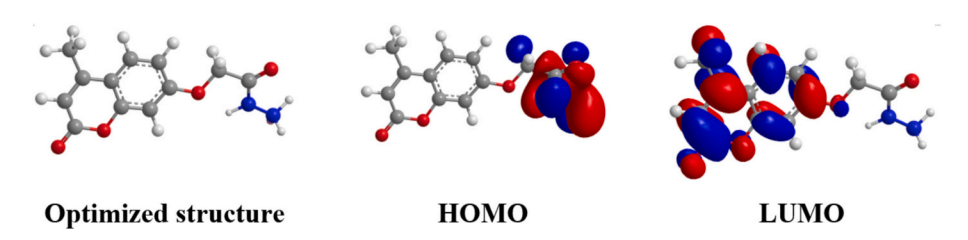


Fig. 7. Optimized structure and Frontiers orbitals.

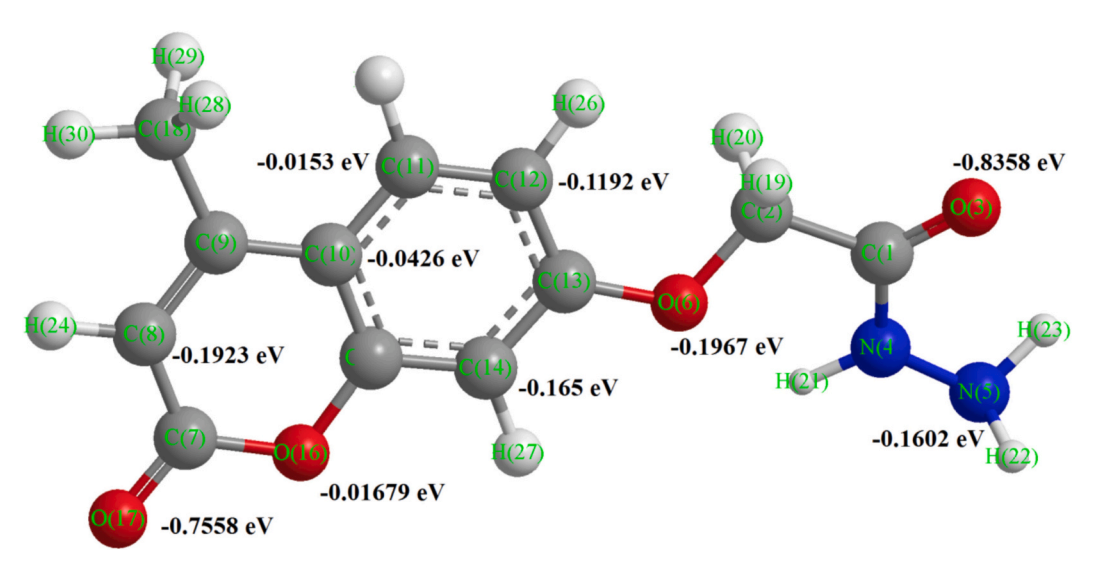


Fig. 8. The atomic charge distribution of AMC inhibitor molecules

performance, as its structural and electronic features allow it to create a durable protective barrier, significantly reducing corrosion [51,52].

3.5. Proposed inhibition mechanism

AMC molecules predominantly adsorb onto the metal surface via chemisorption, forming a monolayer that effectively blocks active corrosion sites. The adsorption behavior follows the Langmuir isotherm, indicating uniform surface coverage without multilayer formation. The adsorbed AMC molecules generate a stable protective layer that limits the diffusion of corrosive species (e.g., Cl⁻ ions) to the metal surface. This layer also significantly reduces anodic iron dissolution and cathodic hydrogen evolution reactions. As the AMC concentration increases, the inhibition efficiency improves due to greater surface coverage. DFT calculations indicate that electron-donating groups in AMC, such as the acetohydrazide moiety, interact strongly with the metal surface, thereby enhancing the inhibitor's efficiency. The electronic properties of AMC, including a small energy gap and high electron density, further support its effectiveness as a corrosion inhibitor [53-55]. Fig. 9 represents the proposed inhibition mechanism which illustrates the adsorption and protective role of AMC on mild steel in 1.0 M HCl solution [56-58].

3.6. A comparison between coumarin derivative and similar works

Table 5 provides a comprehensive comparison of the inhibition efficiencies of AMC and other coumarins tested as corrosion inhibitors for

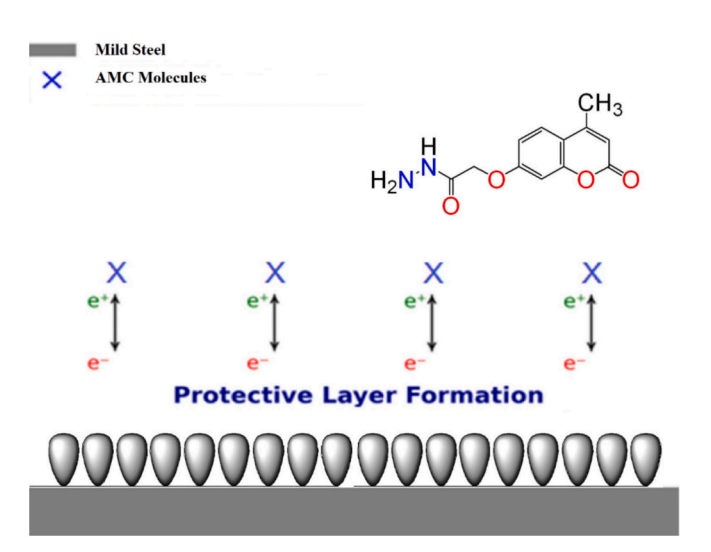


Fig. 9. Schematic Representation of the Inhibition Mechanism of AMC on Mild Steel in 1.0 M HCl Solution.

mild steel in 1.0 M HCl solutions. AMC achieves the highest inhibition efficiency (90.7 %) at a low concentration of 0.5 mM, outperforming other coumarin-based inhibitors. This significant performance is due to its distinctive molecular structure, particularly the acetohydrazide

Table 5Comparison of Inhibition Efficiency of AMC with Other Studied Coumarins.

Compound	Concentration (mM)	Medium	Inhibition efficiency (%)	Reference
a	5 × 10–4 M	1 M HCl	89.2	[59]
b	200 μmol	3 % NaCl	74	[60]
c	200 μmol	3 % NaCl	66	[60]
d	200 μmol	3 % NaCl	87	[60]
e	200 μmol	3 % NaCl	98	[60]
f	200 μmol	3 % NaCl	62	[60]
g	200 μmol	3 % NaCl	92	[60]
h	150 ppm	0.5 M	89.8	[61]
		H_2SO_4		
i	150 ppm	0.5 M	91.5	[61]
		H_2SO_4		
j	150 ppm	0.5 M	93.8	[61]
		H_2SO_4		
k	150 ppm	0.5 M	94.5	[61]
		H_2SO_4		
1	1.0	1.0 M HCl	95.8	[62]
m	0.5	1.0 M HCl	98.8	[63]

(a) N1-(coumarin-7-yl) amidrazone; (b) 4,7-Dimethyl-2H-chromene-2-one; (c)7-Methoxy-4-methyl-2H-chromene-2-one; (d) 7-Hydroxy-4-methyl-2H-chromene-2-one; (e) 7,8-Dihydroxy-4-methyl-2H-chromene-2-one; (f) 7-Hydroxy-4,5-Dimethyl-2H-chromene-2-one; (g) 7-Hydroxy-4,8-Dimethyl-2H-chromene-2-one; (h) 7,7-(propane-1,3-diylbis(oxy))bis(4-methyl-2H-chromen-2-one); (i) 7,7-(1,3-phenylenebis(methylene))bis(oxy)bis(4-methyl-2H-chromen-2-one); (j) 7,7-(1,4-phenylenebis(methylene))bis(oxy)bis(4-methyl-2H-chromen-2-one); (k) 7,7-(naphthalene-2,6-diylbis(methylene))bis(oxy)bis(4-methyl-2H-chromen-2-one); (l) 7-mercapto-4-methylcoumarin; (m) N,N-((2E,2'E)-2,2'-(1,4-phenylenebis (methanylylidene))bis(hydrazinecarbonothioyl))bis(2-oxo-2H-chromene-3-carboxamide) PMBH.

group, which strengthens its ability to form robust coordination bonds with Fe^{2+}/Fe^{3+} ions on the steel surface. This interaction creates a dense and durable protective layer, effectively shielding the metal from corrosive Cl^- ions in the acidic medium.

In comparison, N1-(coumarin-7-yl)amidrazone, achieves a slightly lower inhibition efficiency (89 %) but requires a higher concentration (0.0005 M) [59]. The efficiency of a corrosion inhibitor depends not only on its inhibition percentage but also on the concentration required to achieve this level of protection but also about the concentration at which it achieves this protection. AMC achieves excellent protection (90.7 %) at a low concentration of 0.5 mM, whereas other coumarin derivatives like 4,7-Dimethyl-2H-chromene-2-one (74 %) and 7-Methoxy-4-methyl-2H-chromene-2-one (66 %) require 200 umol, to achieve slightly lower efficiencies. This lower effective concentration of AMC minimizes material usage and cost, further reinforcing its superiority. The structure-function relationship is evident, as compounds like 7,7'-(propane-1,3-diylbis(oxy))bis(4-methyl-2H-chromen-2-one) (89 %) and 7,7'-(1,3-phenylenebis(methylene))bis(oxy)bis(4-methyl-2Hchromen-2-one) (91 %) show moderate efficiencies due to the presence of hydroxyl or methoxy groups, which facilitate moderate adsorption [61]. However, the acetohydrazide group in AMC enhances adsorption through hydrogen bonding and lone pair interactions, resulting in superior inhibition performance. The inhibition efficiency of AMC not only exceeds that of most coumarin derivatives but also rivals other classes of organic inhibitors studied for similar applications. This positions AMC as a promising candidate for both academic research and industrial adoption. AMC exhibits the highest inhibition efficiency (90.7 %) among the listed coumarin derivatives, outperforming even closely related derivatives like 7-mercapto-4-methylcoumarin (95 %) [62]. AMC demonstrates superior efficiency at a lower concentration (0.5 mM), underscoring its enhanced adsorption capabilities. The acetohydrazide functionality in AMC provides additional adsorption sites and strong bonding interactions, making it more effective than simpler coumarins.

In conclusion, AMC demonstrates superior inhibition efficiency, strong adsorption characteristics, and remarkable environmental compatibility compared to similar coumarin derivatives and traditional

corrosion inhibitors.

4. Conclusion

The investigation of AMC as a corrosion inhibitor for mild steel in a 1 M HCl solution demonstrates its high inhibition efficiency, achieving 90.7 % inhibition at a 0.5 mM concentration and 303 K. The adsorption behavior of synthesized inhibitor molecules on the metal surface follows the Langmuir model, indicating the formation of stable and strong bonds between AMC molecules and the mild steel surface. AMC functions as a mixed-type inhibitor, effectively reducing both anodic and cathodic corrosion reactions by forming a protective layer on the tested coupon surface. Theoretical insights from DFT calculations further support the experimental findings, offering a deeper understanding of the corrosion inhibition mechanism. The consistency between experimental results and theoretical data underscores AMC's efficiency as a reliable and potential corrosion inhibitor for mild steel in HCl.

Funding

This research was conducted under the research agreement of Al-Ayen University (AUIQ), funded by the grant code AUIQ-2024-001.

CRediT authorship contribution statement

A.H.A. Kareem: Software, Project administration, Funding acquisition, Formal analysis. **Hakim S. Aljibori:** Conceptualization, Investigation, Writing – review & editing. **Ahmed Al-Amiery:** Writing – review & editing, Writing – original draft, Supervision. **Lina M. Shaker:** Resources, Methodology, Investigation, Formal analysis, Data curation, Conceptualization.

Declaration of competing interest

The authors declare that they have no known competing financial interests or personal relationships that could have appeared to influence the work reported in this paper.

Data availability

Data will be made available on request.

References

- L.M. Shaker, A. Alamiery, W.N. Isahak, W.K. Al-Azzawi, Corrosion in solar cells: challenges and solutions for enhanced performance and durability, J. Opt. 30 (2023 Jun) 1–5.
- [2] A. Alamiery, W.K. Al-Azzawi, Investigation of 3-(1, 3-oxazol-5-yl) aniline as a highly efficient corrosion inhibitor for mild steel in 1 M HCl solution, Int. J. Low-Carbon Technol. 18 (2023) 850–862.
- [3] B. Tan, H. Ren, R. Zhang, R. Wang, L. Ma, X. Li, W. Li, L. Guo, M.K. Al-Sadoon, A novel corrosion inhibitor for copper in sulfuric acid media: complexation of iodide ions with *Benincasa Hispida* leaf extract, Colloids Surf. A Physicochem. Eng. Asp. 20 (705) (2025 Jan) 135710.
- [4] B. Tan, H. Ren, Y. Liu, X. Li, R. Wang, J. Sun, X. Cao, Q. Dai, L. Guo, H. Liu, M.K. Al-Sadoon, Insight into the anti-corrosion performance of crop waste as a degradable corrosion inhibitor for copper in sulfuric acid medium, Ind. Crop. Prod. 15 (222) (2024 Dec) 119654.
- [5] A.A. Al-Amiery, A.Y. Rubaye, A.A. Kadhum, W.K. Al-Azzawi, Thiosemicarbazide and its derivatives as promising corrosion inhibitors: a mini-review, Int J Corros Scale Inhib. 12 (2023) 597–620.
- [6] H.S. Aljibori, O.H. Abdulzahra, A.J. Al Adily, W.K. Al-Azzawi, A.A. Al-Amiery, A. A. Kadhum, Corrosion inhibition effects of concentration of 2-oxo-3-hydrazonoin-doline in acidic solution, exposure period, and temperature, Int. J. Corros. Scale Inhib. 12 (2) (2023) 438–457.
- [7] A.A. Al-Amiery, W.K. Al-Azzawi, Mannich bases as corrosion inhibitors: an extensive review, J. Mol. Struct. 19 (2023 Aug) 136421.
- [8] A.F. Hamood, H.S. Aljibori, M.A. Al-Hamid, A.A. Al-Amiery, W.K. Al-Azzawi, MOP as a corrosion inhibitor for mild steel in HCl solution: a comprehensive study, Progress Color, Colorants Coat. 17 (3) (2024 Jul 1) 207–226.
- [9] M. Taha Mohamed, S.A. Nawi, A.M. Mustafa, F.F. Sayyid, M.M. Hanoon, A.A. Al-Amiery, A.A. Kadhum, W.K. Al-Azzawi, Revolutionizing corrosion defense:

- unlocking the power of expired BCAA, Progress Color, Colorants Coat. 17 (2) (2024 May 1) 97–111.
- [10] A.M. Resen, A.N. Jasim, H.S. Qasim, M.M. Hanoon, A.A. Al-Amiery, W.K. Al-Azzawi, A.M. Mustafa, F.F. Sayyid, Investigating the corrosion inhibition performance of methyl 3H-2, 3, 5-triazole-1-formate for mild steel in hydrochloric acid solution: experimental and theoretical insights, Progress Color, Colorants Coat. 17 (2) (2024 May 1) 185–205.
- [11] H.S. Aljibori, A. Alamiery, T.S. Gaaz, W.K. Al-Azzawi, Exploring corrosion protection for mild steel in HCl solution: an experimental and theoretical analysis of an antipyrine derivative as an anticorrosion agent, Carbon Neutralization 3 (1) (2024 Jan) 74–93.
- [12] I.A. Annon, K.K. Jlood, M.M. Hanoon, F.F. Sayyid, W.K. Al-Azzawi, A. Al-Amiery, Corrosion inhibition of mild steel in HCl solution using MPO: experimental and theoretical insights, J. Mater. 2 (2) (2024) 104–118.
- [13] B.S. Mahdi, H.M. Habeeb, I.A. Aziz, M.M. Hanoon, F.F. Sayyid, A.M. Mustafa, T. S. Gaaz, A.H. Jaaz, A.A. Khadom, E. Yousif, A. Alamiery, Understanding the impact of inhibitor concentration, immersion periods, and temperature on the corrosion inhibition of 2-piperazin-1-yl-1, 3-benzothiazole in HCl solution, Int. J. Corros. Scale Inhib. 13 (2) (2024) 1164–1185.
- [14] A.Y. Rubaye, M.T. Mohamed, M.A. Al-Hamid, A.M. Mustafa, F.F. Sayyid, M. M. Hanoon, A.H. Kadhum, A.A. Alamiery, W.K. Al-Azzawi, Evaluating the corrosion inhibition efficiency of 5-(4-pyridyl)-3-mercapto-1, 2, 4-triazole for mild steel in HCl: insights from weight loss measurements and DFT calculations, Int. J. Corros. Scale Inhib. 13 (1) (2024) 185–222.
- [15] A.A. Al-Amiery, M.A. Fayad, H.A. Hussain, W.K. Al-Azzawi, J.K. Mohammed, H. S. Majdi, Interfacial engineering for advanced functional materials: surfaces, interfaces, and applications, Res. Eng. Des. 16 (2024 Apr) 102125.
- [16] A. Mohammed, H.S. Aljibori, M.A. Al-Hamid, W.K. Al-Azzawi, A.A. Kadhum, A. Alamiery, N-phenyl-N'-[5-phenyl-1, 2, 4-thiadiazol-3-yl] thiourea: corrosion inhibition of mild steel in 1 M HCl, Int J Corr Scale Inhib. 13 (1) (2024) 38–78.
- [17] A.F. Hamood, H.M. Habeeb, B.A. Abdulhussein, A.M. Mustafa, F.F. Sayyid, M. M. Hanoon, T.S. Gaaz, L.A. Hameed, A.A. Alamiery, Weight loss, electrochemical measurements and DFT studies on corrosion inhibition by 7-mercapto-4-methylcoumarin, Res. Eng. Des. 6 (2024 Aug) 102677.
- [18] A.A. Al-Amiery, Y.K. Al-Majedy, A.A. Kadhum, A.B. Mohamad, New coumarin derivative as an eco-friendly inhibitor of corrosion of mild steel in acid medium, Molecules 20 (1) (2014 Dec 29) 366–383, coumarin.
- [19] A.A. Al-Amiery, A. Kadhim, A. Al-Adili, Z.H. Tawfiq, Limits and developments in ecofriendly corrosion inhibitors of mild steel: a critical review. Part 1: Coumarins, Int. J. Corros. Scale Inhib. 10 (4) (2021) 1355.
- [20] D.S. Zinad, Q.A. Jawad, M.A. Hussain, A. Mahal, L. Mohamed, A.A. Al-Amiery, Adsorption, temperature and corrosion inhibition studies of a coumarin derivatives corrosion inhibitor for mild steel in acidic medium: gravimetric and theoretical investigations, Int. J. Corrosion Scale Inhibit. 9 (1) (2020) 134–351, coumarin.
- [21] F.G. Hashim, T.A. Salman, S.B. Al-Baghdadi, T. Gaaz, A. Al-Amiery, Inhibition effect of hydrazine-derived coumarin on a mild steel surface in hydrochloric acid, Tribologia-Finnish J. Tribol. 37 (3–4) (2020 Dec 11) 45–53.
- [22] A.N. Jasim, A. Mohammed, A.M. Mustafa, F.F. Sayyid, H.S. Aljibori, W.K. Al-Azzawi, A.A. Al-Amiery, E.A. Yousif, Corrosion inhibition of mild steel in HCl solution by 2-acetylpyrazine: weight loss and DFT studies on immersion time and temperature effects, Progress Color, Colorants Coat. 17 (4) (2024 Oct 1) 333–350.
- [23] A. Al-Amiery, W.N. Isahak, W.K. Al-Azzawi, Multi-method evaluation of a 2-(1, 3, 4-thiadiazole-2-yl) pyrrolidine corrosion inhibitor for mild steel in HCl: combining gravimetric, electrochemical, and DFT approaches, Sci. Rep. 13 (1) (2023 Jun 16) 9770
- [24] F. Hashim, K. Al-Azawi, S.B. Al-Bghdadi, L.M. Shaker, A. Al-Amiery, Experimental and theoretical approach to the corrosion inhibition of mild steel in HCl solution by a newly coumarin. Sustainability 41 (1) (2019 Nov 14).
- [25] N. Hamdi, A.S. Al-Ayed, R. Ben Said, A. Fabienne, Synthesis and characterization of new Thiazolidinones containing Coumarin moieties and their antibacterial and antioxidant activities, Molecules 17 (2012) 9321–9334, https://doi.org/10.3390/ molecules17089321.
- [26] ASTM, G. G 31–72 American Society for Testing and Materials, 1990. Philadelphia.
- [27] NACE Standard TM 0169/G31-12a, Standard guide for laboratory immersion corrosion testing of metals, 2012.
- [28] A.A.F. Sabirneeza, A novel water-soluble, conducting polymer composite for mild steel acid corrosion inhibition, J. Appl. Polym. Sci. 127 (2016) 3084–3092.
- [29] Gaussian 09, Revision D.01, Frisch, M.J., Trucks, G.W., Schlegel, H.B., Scuseria, G. E., Robb, M.A., Cheeseman, J.R., Scalmani, G., Barone, V., Mennucci, B., Petersson, G.A., Nakatsuji, H., Caricato, M., Li, X., Hratchian, H.P., Izmaylov, A.F., Bloino, J., Zheng, G., Sonnenberg, J.L., Hada, M., Ehara, M., Toyota, K., Fukuda, R., Hasegawa, J., Ishida, M., Nakajima, T., Honda, Y., Kitao, O., Nakai, H.; Vreven, T., Montgomery, J.A., Peralta, J.E., Ogliaro, F., Bearpark, M., Heyd, J.J., Brothers, E., Kudin, K.N., Staroverov, V.N., Kobayashi, R., Normand, J., Raghavachari, K., Rendell, A., Burant, J.C., Iyengar, S.S., Tomasi, J.; Cossi, M., Rega, N., Millam, J. M., Klene, M., Knox, J.E., Cross, J.B., Bakken, V., Adamo, C., Jaramillo, J., Gomperts, R., Stratmann, R.E., Yazyev, O., Austin, A.J., Cammi, R.; Pomelli, C., Ochterski, J.W., Martin, R.L., Morokuma, K.; Zakrzewski, V.G., Voth, G.A., Salvador, P., Dannenberg, J.J., Dapprich, S., Daniels, A.D., Farkas, Ö., Foresman, J. B., Ortiz, J.V., Cioslowski, J., Fox, D.J. Gaussian, Inc., Wallingford CT, 2013.
- [30] T. Koopmans, Ordering of wave functions and eigenenergy's to the individual electrons of an atom, Physica 1 (1933) 104–113.
- [31] A.M. Resen, M.M. Hanoon, W.K. Alani, A. Kadhim, A.A. Mohammed, T.S. Gaaz, A. A.H. Kadhum, A.A. Al-Amiery, M.S. Takriff, Exploration of 8-piperazine-1-ylmethylumbelliferone for application as a corrosion inhibitor for mild steel in

- hydrochloric acid solution, Int. J. Corros. Scale Inhib. 10 (1) (2021) 368–387, https://doi.org/10.17675/2305-6894-2021-10-1-21.
- [32] A.A. Al-Amiery, E. Yousif, W.N. Isahak, W.K. Al-Azzawi, A review of inorganic corrosion inhibitors: types, mechanisms, and applications, Tribol. Industry 44 (2) (2023) 313.
- [33] A.A. Al-Amiery, W.N. Isahak, W.K. Al-Azzawi, Corrosion inhibitors: natural and synthetic organic inhibitors, Lubricants 11 (4) (2023 Apr 11) 174.
- [34] B. Tan, Y. Liu, H. Ren, Z. Gong, X. Li, W. Li, L. Guo, R. Chen, J. Wei, Q. Dai, A. A. AlObaid, N, S-carbon quantum dots as inhibitor in pickling process of heat exchangers for enhanced performance in multi-stage flash seawater desalination, Desalination 23 (589) (2024 Oct) 117969.
- [35] B. Tan, Y. Liu, Z. Gong, X. Zhang, J. Chen, L. Guo, J. Xiong, J. Liu, R. Marzouki, W. Li, Pyracantha fortuneana alcohol extracts as biodegradable corrosion inhibitors for copper in H2SO4 media, J. Mol. Liq. 1 (397) (2024 Mar) 124117.
- [36] B.U. Ugi, J.E. Boekom, P.B. Ashishie, P.U. Ubua, Scopolamine alkaloid as novel green inhibitor of malleable Fe corrosion studied by EIS, DFT, PDP and SEM techniques, Port. Electrochim. Acta 43 (1) (2025) e23–e35.
- [37] H.M. Abubakr, M.E. Ghaith, A.A. El-Sherif, M.S. El-Deab, Influence of metal ions on cysteine as a corrosion inhibitor for low carbon steel in sulfuric acid: polarization, EIS, XPS, and DFT analysis, Int. J. Electrochem. Sci. 19 (7) (2024 Jul 1) 100620.
- [38] Y. Pan, B. Sun, H. Chen, Z. Liu, W. Dai, X. Yang, W. Yang, Y. Deng, X. Li, Stress corrosion cracking behavior and mechanism of 2205 duplex stainless steel under applied polarization potentials, Corros. Sci. 1 (231) (2024 May) 111978.
- [39] V.K. Gattu, J. Obregon, W.L. Ebert, J.E. Indacochea, Effects of open circuit immersion and vertex potential on potentiodynamic polarization scans of metallic biomaterials, npj Materials Degradation 8 (1) (2024 Feb 7) 18.
- [40] Y. He, S. Ren, X. Wang, D. Young, M. Mohamed-Said, B.A. Santos, M.E. Serenario, M. Singer, Temperature dependence of adsorption and effectiveness for a Pyrimidinium-type corrosion inhibitor on mild steel, Corrosion 80 (2) (2024 Feb 1) 177–186
- [41] A.I. Ali, H.E. Megahed, M. Elsayed, A.Y. El-Etre, Inhibition of acid corrosion of aluminum using Salvadore persica, J. Basic Env. Sci. 2 (4) (2024 Oct 1) 110–122.
- [42] A.A. Mahmmod, A.A. Khadom, A.A. Kadhum, A. Alamiery, Quinoxaline as a corrosion inhibitor for copper in nitric acid: kinetics, statistical, and theoretical investigations, Case Studies Chem. Env. Eng. 1 (10) (2024 Dec) 100836.
- [43] R. Haldhar, C.J. Raorane, V.K. Mishra, B. Tuzun, E. Berdimurodov, S.C. Kim, Surface adsorption and corrosion resistance performance of modified chitosan: gravimetric, electrochemical, and computational studies, Int. J. Biol. Macromol. 1 (264) (2024 Apr) 130769.
- [44] D.M. Mamand, T.M. Kak Anwer, H.M. Qadr, Corrosion inhibition performance of organic compounds and theoretical calculations based on density functional theory (DFT), Corros. Rev. 42 (1) (2024 Feb 26) 1–5.
- [45] A. Thakur, A. Kumar, O. Dagdag, H. Kim, A. Berisha, D. Sharma, H. Om, Unraveling the corrosion inhibition behavior of prinivil drug on mild steel in 1M HCl corrosive solution: insights from density functional theory, molecular dynamics, and experimental approaches. Front. Chem. 13 (12) (2024 Jun) 1403118.
- [46] L. Cui, Y. Lv, Y. Dong, H. Liao, S. Wu, X. Li, Benzothiazole-based ionic liquids as environment-friendly and high-efficiency corrosion inhibitors for mild steel in HCl: experimental and theoretical studies, J. Mol. Liq. 15 (394) (2024 Jan) 123769.
- [47] D.M. Mamad, Y.H. Azeez, A.K. Kaka, K.M. Ahmed, R.A. Omer, L.O. Ahmed, The inhibitor activity of some azo compound derivatives using density functional theory and molecular dynamics simulations, Comput. Theoretical Chem. 1 (1237) (2024, Jul) 114645.
- [48] A. Oubihi, M. Ouakki, A. Ech-chebab, E.H. Assiri, K. Tarfaoui, M. Galai, M. E. Touhami, M. Ouhssine, Z. Guessous, Corrosion inhibition in 1M HCl of mild steel with Thymus leptobotrys Murb essential oil (TLMEO): electrochemical measurements and density function theory (DFT) and molecular dynamics (MD) simulations, J. Appl. Electrochem. 54 (6) (2024 Jun) 1279–1297.
- [49] A. Roua, A.A. Hassani, A. Fitri, A.T. Benjelloun, M. Benzakour, M. Mcharfi, K. Tanji, Adsorption studies of isoxazole derivatives as corrosion inhibitors for mild steel in 1M HCl solution: DFT studies and molecular dynamics simulation, J. Mol. Model. 30 (6) (2024 Jun) 1–6.
- [50] K. Shalabi, H.M. Abd El-Lateef, M.M. Hammouda, M.M. Rashed, The anticorrosive efficacy of newly synthesized Pyrido-bis (benzo [b] azoninone) analogs on carbon steel under sweet corrosive environments: a combined empirical and theoretical approaches, Colloids Surf. A Physicochem. Eng. Asp. 30 (2024 Jul) 134958.
- [51] K. Mortadi, A. El Amri, M. Ouakki, R. Hsissou, A. Jebli, A. Lebkiri, Z. Safi, N. Wazzan, A. Berisha, M. Cherkaoui, E.M. Hbaiz, Electrochemical and theoretical studies on a bioactive *Juniperus oxycedrus* essential oil as a potential and ecofriendly corrosion inhibitor for mild steel in 1.0 M HCl environment, Inorg. Chem. Commun. 15 (2024 Feb) 112196.
- [52] M. Naciri, S. Skal, Y. El Aoufir, M.R. Al-hadeethi, H. Lgaz, H. Bidi, M. El Moudane, A. Ghanimi, A. Bellaouchou, Unveiling the influence of furan and thiophene on the corrosion inhibition capabilities of novel hydrazones derivatives in carbon steel/ HCl interface: a dual experimental-theoretical study, Colloids Surf. A Physicochem. Eng. Asp. 5 (686) (2024 Apr.) 133272.
- [53] B. Ran, Y. Qiang, X. Liu, L. Guo, A.G. Ritacca, I. Ritacco, X. Li, Excellent performance of amoxicillin and potassium iodide as hybrid corrosion inhibitor for mild steel in HCl environment: adsorption characteristics and mechanism insight, J. Mater. Res. Technol. 1 (29) (2024 Mar) 5402–5411.
- [54] Y. Qiang, L. Guo, H. Li, X. Lan, Fabrication of environmentally friendly losartan potassium film for corrosion inhibition of mild steel in HCl medium, Chem. Eng. J. 15 (406) (2021 Feb) 126863.
- [55] Y. Qiang, H. Zhi, L. Guo, A. Fu, T. Xiang, Y. Jin, Experimental and molecular modeling studies of multi-active tetrazole derivative bearing sulfur linker for protecting steel from corrosion, J. Mol. Liq. 1 (351) (2022 Apr) 118638.

- [56] K. Jrajri, M. El Faydy, M. Alfakeer, S.S. Al-Juaid, Z. Safi, I. Warad, F. Benhiba, D. R. Bazanov, N.A. Lozinskaya, M. Abdallah, A. Zarrouk, Correlation between molecular structures and performance of corrosion inhibition of carbon steel by some imidazole analogs in HCl 1 M: integrating practical and theoretical aspects, Colloids Surf. A Physicochem. Eng. Asp. 5 (700) (2024 Nov) 134683.
- [57] N. Timoudan, A. Titi, M. El Faydy, F. Benhiba, R. Touzani, I. Warad, A. Bellaouchou, A. Alsulmi, B. Dikici, F. Bentiss, A. Zarrouk, Investigation of the mechanisms and adsorption of a new pyrazole derivative against corrosion of carbon steel in hydrochloric acid solution: experimental methods and theoretical calculations, Colloids Surf. A Physicochem. Eng. Asp. 5 (682) (2024 Feb) 132771.
- [58] A.R. Eltohamy, M.M. Kamel, A. Aboelmagd, S.M. Rashwan, A.S. Fouda, M.K. Awad, F.M. Atlam, 'Insights into using a Schiff base as corrosion inhibitor for carbon steel in HCl medium: experimental and theoretical approaches'. Catrina: the, Int. J. Environ. Sci. (2024 Jun 19) 25–39.
- [59] L. Raisemche, I. Kaabi, T. Douadi, M. Al-Noaimi, A. Alrashed, M.S. Mubarak, N. Elboughdiri, A. Zouaoui, Y. Benguerba, Corrosion inhibition of mild steel in

- acidic environments: mechanistic insights and protective effects of azo-cum inhibitor, J. Environ. Chem. Eng. 12 (2) (2024 Apr 1) 112354.
- [60] I. Semic, S.C. Zeljkovic, The influence of some 4-methylcoumarins on the electrodeposition and characteristics of zinc coating, Prot. Met. Phys. Chem. Surf. 51 (1) (2015) 131–137.
- [61] M. Abd El-Raouf, E.A. Khamis, M.T. Abou Kana, N.A. Negm, Electrochemical and quantum chemical evaluation of new bis (coumarins) derivatives as corrosion inhibitors for carbon steel corrosion in 0.5 M H2SO4, J. Mol. Liq. 255 (2018 Apr 1) 341–353.
- [62] A.F. Hamood, H.M. Habeeb, B.A. Abdulhussein, A.M. Mustafa, F.F. Sayyid, M. M. Hanoon, T.S. Gaaz, L.A. Hameed, A.A. Alamiery, Weight loss, electrochemical measurements and DFT studies on corrosion inhibition by 7-mercapto-4-methylcoumarin, Res. Eng. Des. 1 (23) (2024 Sep) 102677.
- [63] A.A. Kadhum, A.B. Mohamad, L.A. Hammed, A.A. Al-Amiery, N.H. San, A.Y. Musa, Inhibition of mild steel corrosion in hydrochloric acid solution by new coumarin, Materials 7 (6) (2014 Jun 5) 4335–4348.